BULLETIN OF THE POLISH ACADEMY OF SCIENCES
TECHNICAL SCIENCES, Vol. 73(4), 2025, Article number: e153432
DOI: 10.24425/bpasts.2025.153432

Modeling responsive structures under external forces using an evolutionary algorithm

Szymon JANKOWSKI* **and Waldemar BOBER**

Faculty of Architecture, Wroclaw University of Science and Technology, Wybrzeże Wyspiańskiego 27, 50-370 Wrocław, Poland

Abstract. The design of responsive structures has evolved significantly, establishing itself as an interdisciplinary field characterized by a fully customized ideation process. In order to streamline and unify this process, a novel method for modeling the behavior of rod-like responsive structures using an evolutionary algorithm is introduced. The proposed mathematical framework leverages key geometric and physical parameters to control the generative process, enabling adaptability and fluidity in form development. By employing an evolutionary algorithm, the method offers an alternative to conventional rigid and repetitive morphing models, providing flexibility and innovation in responsive design outcomes. The model developed supports independent learning and fosters originality in solutions at both architectural and urban scales. Moreover, the presented methodology serves as the foundation upon which the authors developed the model, enabling its application across a wide spectrum of responsive structures for users. This paper addresses challenges in spatial modeling, behavioral algorithms, and the implementation of responsive architecture, presenting the authors' innovative model for rod-like responsive structures alongside performance analysis. The methodology demonstrates promising results in terms of adaptability and efficiency, with potential for further refinement to enhance speed and output quality. The study also describes challenges and risks for further development of responsive models implementation.

Keywords: responsive architecture for urban planning; shape changing structures; morphing urban structures; smart city structures; evolutionary algorithm; structure behavior modeling.

1. INTRODUCTION

Responsive architecture in modern form has been proposing solutions introducing autonomous movement into structures since the 1950s. Initially, these concepts were strictly theoretical (as in [1]), but with technological advancements, practical solutions for responsiveness also emerged. Early concepts of residential structures resembling machines and achieving at least a minimal level of responsiveness did not meet a satisfactory number of implementations. Outside of the research, there are no examples of the use of responsive structures in public spaces but from the beginning the idea of responsiveness was assigned to social and public districts such as moving blocks of flats or exchangeable spaces. Kinetic facades and lightweight membrane structures with controlled tension parameters are excluded from this list of realizations. Attempts to translate innovative designs into spatial forms encountered practical difficulties and issues related to the scale of forces and weight, particularly in shifting from static to dynamic structures, as noted in many studies and extensively in the [2].

There are architectural designs featuring structures with movable elements. The most prominent examples include retractable roof systems or entirely sliding structures, like those described in [3]. However, these lack responsiveness integrated with more versatile movements and greater autonomy of operation and, moreover, with overcoming scaling problems for creating fully responsive human areas. The role of such responsive systems has been partially adopted by kinetic façades [4], which cannot be classified as responsive structural systems due to their lack of adequate load-bearing capabilities. In these cases, only a lightweight substructure is movable, highlighting the first challenge of the concept of responsiveness, namely, the scale and range of forces within which these currently theoretical structures operate in contrast to widely implemented movable installations.

This issue becomes particularly evident in the field of biomimicry, particularly in study [5], where solutions are almost entirely inapplicable to responsive structural systems.

Past studies on responsive structures have primarily focused on the simplest structural systems to which responsiveness can be applied. These include lightweight structures such as trusses [6] and tensegrity systems [7], often differentiated based on the implementation of actuators in either parallel or longitudinal configurations, as distinguished by Senatore *et al.* [8]. Over time, these explorations have led to unique solutions specific to responsive architecture, such as the "infinite stiffness structures" described and evaluated in [9]. The diversity in behavior and the scale of structural shape changes resulted in the distinction between small shape changes and large changes. Still, there is a gradual shift away from the original spatial responsiveness of a system (seen in the 1970s and 1980s) to the individual adaptability of elements within urban systems, which is losing its ability to autonomously change structure in favor of fragmented individually designed objects.

Simultaneously, research has explored practical implementation possibilities by proposing specific design solutions, as

*e-mail: szymon.jankowski@pwr.edu.pl

Manuscript submitted 2024-10-18, revised 2025-01-11, initially accepted for publication 2025-01-11, published in July 2025.

outlined in [10]. Conversely, an alternative approach has focused on refining analytical models to better simulate structural movements, enabling the development of architectural systems capable of achieving the intended range of shape changes.

A new field is the implementation of responsiveness in continuous shell and monolithic structures, where precise control of stress distribution is sacrificed in favor of enhanced safety margins, mostly evaluated and described by Senatore *et al*. in [11] and other works in the series. Responsiveness implemented into a load-bearing structure involves a significantly broader set of issues.

Simultaneously with practical implementation challenges, theoretical issues are also being addressed. Behind every responsive structure lies a system responsible for supervising and determining geometric changes. Initially, the foundation of such systems was in the form of simple machine learning algorithms and fuzzy logic methods (e.g. to maintain structure deflection control in [12]). With technological advancements and increased computational power, form-finding simulation techniques began to be employed. This is particularly noticeable at the urban scale, where original concepts like the "movable theater", intended to promote responsiveness of the entire city in the form of movement, have been superseded by more easily segmented and staged solutions of responsiveness of infrastructure, communications and ICT, losing the architectural aspect.

The most widely adopted approach, due to its computational reliability and efficiency, involves rigid optimization formulas based on selected structural and static parameters influencing the performance of the system as shown in [13], allowing for instantaneous system response to external force changes. Most of the current rigid algorithms focus on minimizing embodied energy like [13] for structure material efficiency enhancement. Separately, the structural system and its topological optimization are developed – both in terms of creating software for topology analysis and optimization, as well as applying and interpreting the results to achieve the aforementioned total energy minimization, as proposed in [14].

A diversification of challenges is observed in relation to entirely general approaches to optimizing the design process of responsive structures. Issues such as structural safety and the degree of force control and measurement within individual elements are also being addressed.

The increasingly complex interdisciplinary nature of the topic demands closer project cooperation between architecture, structural engineering, electronics, programming, as well as contractors and suppliers of materials and technologies. Traditional design methods are insufficient for the implementations being discussed, necessitating the development of a unique design process each time. A framework presented in [15] serves as one example of such a design approach. The complexity of the issues that need to be addressed during the design phase dictates the highly individualized nature of work on kinetic structures, a trend that is gaining popularity [16].

An additional challenge in implementing responsiveness is the lack of software dedicated strictly to structures that react to external stimuli through geometry changes. Industry-standard software such as Archicad, Microstation or Revit allows for volatility in buildings, but this functionality remains beyond affordability due to the need to develop custom programs and motion management code from scratch. Current projects on computerization and automation of movement integration in architecture remain in the research phase, such as the complex and challenging-to-develop idea of VR architecture described in [17], with the most accessible approach being the adaptation of common software solutions to incorporate parameters of variability conditioned by time or specific stimuli.

To illustrate an approach to modeling responsive structures, the authors present a method for shaping architectural forms with a time-dependent variability parameter. This approach addresses fundamental static issues and design possibilities. The method for modeling responsiveness in architectural structures was developed using Rhinoceros 8 with the Grasshopper plugin, extended with Galapagos, Karamba 3D, and LunchBox modules. The model analyzes motion in terms of discretized positions and reduces the need for manual control, simplifying and securing the conceptual design process. It also allows for implementing conditions and constraints that users can define or modify within the project. Additionally, the authors present basic methods for applying geometric boundaries using mathematical formulas.

Past applications of the research tool combining functionalities of Karamba 3D and Grasshopper primarily involved simple static optimizations of structures in specific construction cases, utilizing cross-section optimization and analyzing force flow to define optimal reinforcement patterns that can be found in [18]. Some studies focused on employing form-finding methods using the Kangaroo module. Dynamic research was based on passive analysis of the behavior of deformed structures, without user intervention in their geometry (like in [19]), without real time adaptivity. Both simple and complex shape modifications and optimizations are conducted using various formulas and methods such as geometry and topology optimization, which leads to a strict final resultant structure in [20].

The model's functionality is based on its parameterization. The looping shape modification process controlled by feedback creates artificial dynamics in structure using an evolutionary algorithm (Fig. 1).

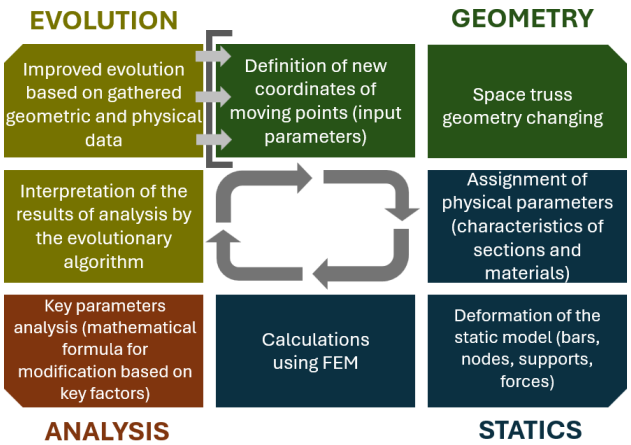

Fig. 1. Looping model diagram. Consecutive iterations generate results based on an expanding database

The phase of analyzing current geometry generates information for algorithm, which then selects vectors of changes for input parameters. These parameters are the coordinates defining the surfaces on which responsive structure is formed. With each iteration of the structure's form, the model seeks increasingly efficient solutions based on a growing pool of analyzed geometries. The key is to develop a mathematical formula that ties all significant geometrical parameters together, considering their importance and interrelations while avoiding excessive fluctuations in modification function [21].

The paper, focusing on the presentation of the authors' solution of the mathematical formula of modification for the evolutionary algorithm, presents the most general approach to modeling responsive structures in order to simplify the process of initial formation of ideas in responsive architecture. By using the evolutionary algorithm in this way, the authors allow for the autonomous generation of unique geometrically efficient solutions in place of the existing rigid resultant geometries in a controlled manner. This gives the possibility to increase the autonomous work of responsive structures and their independent development, helps design and realize more complex urban and social architecture that functions as part of a global complex system instead of individualized research. Moreover, as the beginning of further realization steps, the paper also presents the model and simulation tests of authors expanding bar design for real physical structure that encounters difficulties of realization.

The results of efficiency tests for the formula developed are presented, followed by improvements made to the formula to enable faster attainment of satisfactory outcomes. Future research directions, identified limitations and challenges in implementing the model across diverse structures are also discussed.

2. DESIGN MODEL

2.1. Geometry

The first stage of the process involves defining a type of structure and its base geometry. To reduce complexity of static calculations, a truss structure with square grids offset by half a cell was used. Square base shape and geometry with four axes of symmetry simplify the process of validating measurement results and optimization by enabling usage of force interpolation principles and symmetry of results. Search for structural forms for complex load cases is to be addressed by applying superposition based on elementary cases. Structure is curved in two surfaces, maintaining all symmetry axes for reference shape.

In the first stage of creating a model, the goal was to construct a surface describing curvature of truss grids. Different methods of creating geometry allowed for different degrees of manipulation of the structure's shape, depending on the complexity of describing surfaces and curves or points that form them. Rate of the shape modification process is closely linked to complexity of surface description, as the algorithm must account for more dependencies between variables. An optimal solution is to use a minimal number of parameters while maintaining maximum control over each element of the structure's geometry. Form design was based on NURBS curves defined by 3 points and a second degree of freedom, ensuring smooth curvature of curves and, consequently, entire surface in all directions.

The model was constructed based on 8 points evenly distributed along the perimeter of a square with sides of 10 meters in length. Points were located at the corners and midpoints of edges. Curvature of edges was achieved by varying positions of points along the z-axis (Fig. 2).

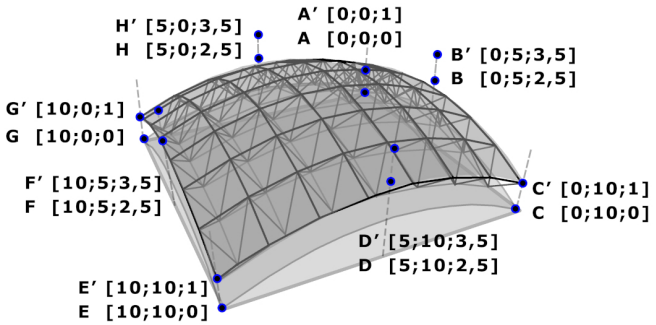

Fig. 2. Surfaces generated by 8 NURBS curves using 16 control points form entire motion framework for truss spanning between them

The "Edge Surface" method was used to determine the surface defined by specified curves, resulting in a spherical segment shape. The second surface was modeled in the same manner, but its points were defined by offset vectors relative to the points forming the first surface. All points on surface 2 were located 1 meter above the points of the lower surface. The same "Edge Surface" method was used to create a top surface from offset points.

Boundaries for translations of all coordinates of each point were defined to allow movement of structure simultaneously, preventing uncontrolled displacements and creation of self-intersecting geometry. During the study, only the "z" coordinates of edge midpoints were controlled, resulting in a set of 8 variables influencing the entire geometry except for corners, which serve as support locations.

A spatial truss was spanned on modeled surfaces using the "Space Truss Structure 2" method from LunchBox add-on (Fig. 3).

This function generates a structure where lower nodes are positioned on the first surface and upper nodes on the second. In addition to nodes, the function defines the lines representing

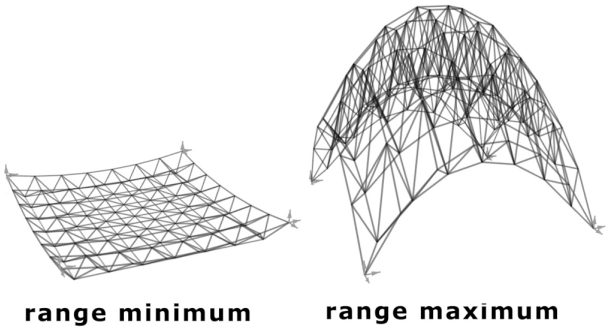

Fig. 3. Visual representation of the structure's range of motion. All intermediate forms are achievable

axes for struts. The method is further defined by parameters for a number of grid divisions in both directions parallel to the adjacent side edges. In the study, these values were set to a 7-part division in both directions. The method automatically calculates node points, creating equal divisions of individual polylines. As a result, the method provides data on the coordinates of all translated nodes, lines connecting to and from the nodes, and their lengths. Choice of truss topology is followed by its potential to achieve the most efficient results in terms of the object's mass and relatively simple geometry as examined in Kaveh *et al.*'s research [22].

2.2. Statics

Defining the physical parameters required for static calculations and processing calculations themselves was accomplished using the Karamba 3D add-on. In the first stage, bars, nodes, supports and applied forces were defined. Elements were then combined into a complete computational model and enhanced with modules for analysis, cross-section optimization as well as graphical and digital presentation of static calculation results.

Data for all lines as an axis in the model were connected to the cross-section defining module, assigning the necessary physical and geometric properties to them. A ring-shaped cross-section with fixed diameters was chosen from among two variants. In the first one, diameter and wall thickness of cross-section were slightly oversized to increase the set of spatial solutions meeting the load-bearing condition during motion modeling. In the second variant, geometry data were provided within a range far from realistic values. A detailed description of this methodology is found in the analysis-weight section. Minimizing the cross-section forms part of the final stage of the structural calculation process, occurring only after the motion system has been established, and it is not included in the study. Along with the cross-section, the construction material was defined, selecting AW8011AH26 aluminum from the predefined program list. Every bar was defined as a hollowed steel circular bar with an external diameter of 15cm and wall thickness of 1 cm.

In each of the four corners of the lower grid of the structure, non-movable rotational supports were placed. This stiffening, while maintaining the freedom of supports rotation in all directions, is essential for enforcing geometry changes when bars are lengthened or shortened.

In the next step, forces are applied to the structure. Each time, a single static system of external forces is analyzed, to which the structure adapts its shape through dynamic changes in its geometry. Thus, the correct design of the studied cases reduces analysis time of the entire structure. A constant force present in all studies is gravity, acting with the Earth's gravitational acceleration of 9.98 m/s^2, relative to the global coordinate system of the project. The key element affecting geometry change is additional forces applied to designated nodes in the structure. Concentrated forces are specified at designated nodal points, while distributed forces are automatically divided by program among all nodes subject to a given force within the defined area, considering the force-to-surface fragment ratio for each construction node. Direction of forces, their magnitudes and points of application were all defined. In the study being described, simple load cases with one and two concentrated forces and basic cases of distributed forces were analyzed to examine the model's potential for generating efficient geometries.

Bars, nodes, supports and forces contributed to the computational model, which was identified by the program as a unified structure. Calculations were conducted using a simplified finite element method (FEM), dividing all structural elements into several parts. In this study, each bar was divided into four smaller elements. This level of precision is sufficient for truss calculations, although for a continuous structure, such as e.g. a shell, a higher number of divisions would be necessary. Its complexity parameter is adjustable from user-software level as a regular variable.

The stage of recalculating the structure considers maximum stress on cross-section and displacements. If any value is exceeded, the cross-section of the overloaded bar is switched to a more durable one, which in the study was programmed to generate an inefficient structure. The maximum stress was arbitrarily set at 90%, while the displacements were calculated by a module that determines the span of the structure as the longest distance between two adjacent supports. The value calculated is then divided by a manually selected coefficient, set in the study as 300. This value for the structure has been defined as for an analogous construction according to Eurocode 1993-1-1 in the national annex for Poland for structures with a roof function that does not affect sensitive elements of the structure. The resulting value represents the maximum allowable displacement, enabling control of the structure even when the support location is changed, or the support is moved.

After calculating internal forces and obtaining static results, the program proceeds with the visualization of results. The first module is responsible for presenting geometry deformation in the form of model displacements. The second module displays data on the rate of bar utilization and stress values, presenting them graphically on the deformed model and as numerical values assigned to respective structural elements.

2.3. Analysis

Shape modification of subsequent truss iterations is based on analysis results. Truss modeled with the initial parameters described serves as the reference model. All subsequent shapes obtained during the modeling process are evaluated against this reference system. To automate the process of adapting geometry to the current configurations of external forces, an evolutionary algorithm was incorporated. This algorithm manages the structural form's variability over time by searching for evolutionary directions that lead to increasingly efficient shapes. The system collects data from each iteration to progressively refine the framework for defining the most efficient solutions. Upon every change in external load conditions, the system resets the existing solution pool, restarting the evolutionary algorithm to gather new data on evolution directions and effective forms. Changes in external conditions during simulation are defined as any non-zero change in the force's direction or magnitude. For physical models, instead of any minimal difference, a measurement accuracy threshold should be defined, with deviations beyond this threshold marking a change in the conditions. This

would slow down environmental condition changes, allowing the system enough time to find efficient geometry and respond. During each iteration, the algorithm compares the result of the optimization function with the previous and best results so far. The algorithm used in this study is guided by a mathematical definition of structural efficiency and geometric complexity. This function, composed of several coefficients, is sensitive to changes in shape, element lengths and stress distributions. It signals a drop in efficiency by increasing in value. Consequently, the algorithm is configured to minimize the modification function.

Building the research model relies on accurately defining the most critical data for structure analysis. For static structures, primary criteria include mass, construction and management costs that are the field of study in [23], or structural topology explored deeper in [24]. Additional execution and functional parameters are associated with kinetic structures that are exampled by [25] inventions. However, each time, the process of selecting key parameters is individualized. The method developed in this paper constitutes a framework rather than a ready-made solution.

Since the employed algorithm does not manage results of multi-criteria modifications, all parameters and properties of the construction considered critical were consolidated into a single equation formulated from appropriately weighted additive elements. These parameters pertained to geometric properties, statics and prototyping constraints, which the authors defined as significant at this stage.

$$V_{\text{opt}} = \sum_{x=a}^{g} x, \tag{1}$$

V_{opt} – final value of the structural optimization coefficient.

Elements of the optimization function:
a – deflection arrow in micrometers,
b – structural mass in kilograms,
c – cross-section utilization degree,
d – bar utilization ratio,
e – bar extension ratio,
f – bar length ratio,
g – intersection of the upper and lower grid surfaces.

The inability to introduce geometric constraints such as maximum rod extension or minimal cross-sectional utilization directly into the computed model necessitated the use of mathematical restrictions and structural penalization methods. These measures aimed to achieve a model with the desired static properties while maintaining a geometry that is as simple as possible to realize. The minimal set of parameters in the function prevents the algorithm from artificially generating efficiency by focusing on a single parameter, which could result in the creation of non-drawable forms and hinder the physical construction of the structure based on the obtained geometry. Therefore, the function incorporates elements that ensure its correctness, ease of execution and physical handling of the construction, as well as the efficiency of the structure's shape.

The development of the mathematical framework for managing the generation phase of the most efficient geometries results in a two-stage process. The first stage, which defines the key measured parameters, required specifying weights and value limits for each criterion in the result. The second stage involved examining the behavior of the resulting function and refining it to include the desired relationships between the values of the various criteria to improve its efficiency.

The overall function of the efficiency formula is to achieve the best adjusted geometry according to actual load case with minimal geometry changes.

2.3.1. Displacement

Improving the efficiency of construction's utilization by introducing a geometry modification system aimed to increase the range of maximum loads that can be applied to the structure or reduce cross-sections of members, thereby relieving the structure and making it straighter and cheaper to construct. Due to the lack of research on the reliability of responsive structures, it is not feasible to design constructions that meet load-bearing requirements only with the use of active telescoping systems, as potential system failures could lead to construction collapses. However, it is possible to design structures modified to account for serviceability limits, without risking structural collapse in the event of a failure. According to the method's assumptions, the modification function considers the deflection of the structure by calculating maximum vertical displacement among all nodes of the construction.

2.3.2. Weight

Weight parameter is not a direct indicator of shape efficiency, although in static optimizations, it is one of the main modification criteria. It validates the static solutions proposed by the algorithm. A basic ring-shaped cross-section of a rod with a diameter of 15 cm and a wall thickness of 5 cm, designed to withstand a uniform structure for the entire assembly, was defined, along with an additional cross-section with unrealistic parameters of a 10 000 cm diameter and a 50 cm wall thickness, thereby increasing its weight. Weight of structure plays a crucial role in verifying correctness of the solution.

With each geometric change, the program recalculates the structure, stresses and moments, and then, based on these, selects appropriate cross-sections from a predefined list provided by the user. If utilization value for proper diameter remains below the imposed maximum utilization threshold of 90%, the program assigns all cross-sections as regular ones of 15 cm in diameter. In such a situation, the total weight of the structure oscillates between 7500 kg and 8000 kg, influencing the optimization function in an imperceptible way. However, if even a single rod exceeds the established load-bearing limit, cross-section is replaced with an unrealistic cross-section element, increasing weight by 3 to 4 orders of magnitude. Such a surge in value distorts the modification function result, positioning the geometry obtained insignificantly in the result geometries collection. Such variation in cross-sections and the use of unrealistic geometry in one case allows the algorithm to focus only on generating statically correct structures that are within the strength limits. An alternative to an unrealistic cross-section for overloaded bars could be to manually introduce a formula

that, upon detecting too high utilization of any bar, would add a significant sum of points to the optimization function, making the given solution inconsiderable.

2.3.3. Utilization rate of the section

Cross-sectional utilization is one of the direct shape modifiers, referring to the efficiency of structural use. Each rod in the structure is examined for how much the construction utilizes the rod's maximum load-bearing capacity. All rods are then assigned to one of several categories. Optimal cross-sectional utilization is within the 50–60% range, where the penalty coefficient is the lowest. As parameter value deviates from this optimal range, the penalty coefficient increases.

Algorithms simultaneously monitor two factors. The primary function is to detect sets of overloaded rods. If their number in the structure is large, optimization function reaches an inefficient value, and the algorithm deems iteration as insignificant. Additionally, the algorithm aims to maintain a uniform distribution of stress within the structure.

$$\text{for } (0 \le w < 0.5), \quad c_x = (0.5 - w) \cdot 1000, \tag{2}$$

$$\text{for } (0.5 \le w < 0.6), \quad c_x = (0.6 - w) \cdot 100, \tag{3}$$

$$\text{for } (0.6 \le w < 0.7), \quad c_x = (0.7 - w) \cdot 500 + 100, \tag{4}$$

$$\text{for } (0.7 \le w < 0.8), \quad c_x = (0.8 - w) \cdot 2000 + 600, \tag{5}$$

$$\text{for } (0.8 \le w < 0.9), \quad c_x = (0.9 - w) \cdot 10000 + 2600, \tag{6}$$

$$c = \sum_{x=1}^{392} c_x, \tag{7}$$

w – cross-sectional utilization, ranging from 0.0 to 0.9. The coefficient is calculated as a positive value of cross-sectional utilization, using the same mathematical formula for both compression and tension,

x – rod number in the structure (there are 392 rods in the analyzed model),

c_x – value of the parameter of use of a single bar in the structure.

Penalty coefficients and ranges provided in the formulas were adjusted by the authors based on preliminary measurements of the average utilization of structural elements. These should be adjusted each time according to the type of construction and cross-sections of elements used.

2.3.4. Proportion of cross-sections utilization

In addition to the data on the overall utilization coefficient of the bars, the ratio of the most stressed to the least stressed bar cross-sections was also considered. The study used only two cross-sections, which can be non-optimal, but this did not affect the comparative results between successive geometry iterations.

A direct comparison of the maximum to minimum values would not prove meaningful. Applying force at one corner of the structure impacts bar stresses at the opposite end to a significantly different degree than a force applied near the center of the structure. The solution to this problem was to rank utilization coefficients of all bars in ascending order and determine the values for the lower 20th percentile and the upper second percentile. The disparity in centile values stemmed from the corresponding disparity in cross-section utilization. Most of the models consist of elements with minimal usage since it is impossible to consistently distribute stress evenly while maintaining economical structural geometry.

$$d = \frac{w_{98}}{w_{20}} \cdot 100, \tag{8}$$

w_{20} – bar utilization factor with a centile of 20%,
w_{98} – bar utilization factor with a centile of 98%.

The formula prevents overloading the structure in one direction or distributing stress across an inefficient number of elements. This distribution could impact reliability of the structure, which, when working with a limited number of bars, would become more susceptible to sudden exceedances of load-bearing limits.

2.3.5. Bars elongation

Elongation refers to the execution issues of the physical model of the structure. The design assumes usage of a proprietary system of extendable rods capable of adjusting their extension to accommodate required changes in geometry. Currently, there are no spatial truss systems available that can serve as ready-made solutions for such an application [26].

For purposes of this study, a model of a telescopic rod was designed to address the lack of available system solutions. Stiffness and statics of the model across the full spectrum of target positions are crucial to the behavior of the structure and required numerical verification. The rod's performance characteristics were determined using the finite element method (FEM). A complete single rod model was designed in Autodesk Inventor 2024. Stress analysis was conducted in Autodesk Nastran, examining the reduced stresses under constant forces of 100 N axially applied at both ends of the rod for various extension configurations.

The telescoping function assumes a maximum elongation of 15% of the rod's base length, which significantly limited the ability to generate structural shapes but maximized stability. In the conducted study, 17 stress measurements were performed, and results were collected in a graphical representation to illustrate trends in measured values.

The results, presented in two scales (Fig. 4a, b), show a trend resembling linearity. Maximum stress values, collected in the first graph, consistently occur at connection of diagonal brace with its corresponding wing at bolted joint. Key stress values, depicted in Fig. 4c, d, were measured on diagonal braces that are most susceptible to buckling or twisting. The threshold for the safest elongations range is up to 8% of length, which exhibit greatest linearity, excluding any notable impact from additional destructive phenomena within this range.

Maximum elongation of 15% of length, determined to remain within acceptable system stiffness limits, can be increased but requires further strength testing or modifications to the movement mechanism. Furthermore, the rod design presented allows for construction of spatial structures analogous to the studied

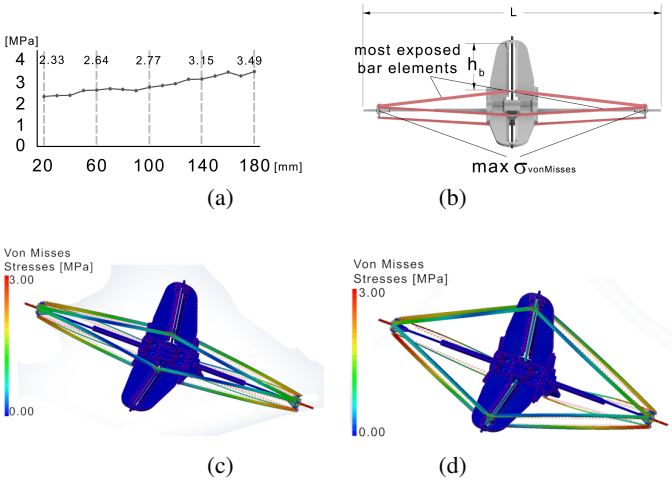

Fig. 4. (a) Maximum stress in the struts of the bar in MPa, with respect to length hb. (b) Telescopic rod model according to the authors' study. (c) FEA results for the case of extreme rod extension. (d) FEA results for the case of extreme rod shortening

truss model, ensuring access to all construction elements during assembly and maintenance through designed lifespan of the structure. Rods with greater elongation, due to their increased size, would negatively impact ease of implementation and use in constructions. To simplify structural analysis in Rhino, the complex geometry of the rod designed in Inventor was replaced with a prism-shaped rod of tubular cross section, simplifying its behavior while maintaining the parameters outlined in Section "2.2. Statics". The overall mass of idealized bars (20 406 kg) is like a detailed model (20 411 kg). The need to artificially define buckling behavior was avoided due to appropriately low stress values and the telescopic rods resistance to this phenomenon within the specified extension range of up to 15%.

Further assumptions specified that there were no misalignments in the structural element assembly. While no manufacturing imperfections were defined in the computational model, a physical structural model would require additional analysis to determine the necessary manufacturing precision and the impact of inaccuracies on the structure's performance.

Based on the collected static analysis data for the parameter governing the degree of rod extension, the following ranges and penalty values for the algorithm's function were determined.

$$\Delta l = \frac{l_o}{l_b}, \tag{9}$$

$$\text{for} \quad (\Delta l < 0.85), \quad e_x = (\Delta l - 1) \cdot 10000, \tag{10}$$

$$\text{for} \quad (0.85 \leq \Delta l < 0.92), \quad e_x = (\Delta l - 1) \cdot 1000, \tag{11}$$

$$\text{for} \quad (0.92 \leq \Delta l < 1.0), \quad e_x = (\Delta l - 1) \cdot 200, \tag{12}$$

$$\text{for} \quad (1.0 \leq \Delta l < 1.08), \quad e_x = (\Delta l - 1) \cdot 200, \tag{13}$$

$$\text{for} \quad (1.08 \leq \Delta l < 1.15), \quad e_x = (\Delta l - 1) \cdot 1000, \tag{14}$$

$$\text{for} \quad (1.15 \leq \Delta l), \quad e_x = (\Delta l - 1) \cdot 10000, \tag{15}$$

$$e = \sum_{x=1}^{392} e_x, \tag{16}$$

l_b – length of rods in reference static structure,
l_o – length of rod after adjustment for elongation,
Δl – proportion of rod elongation relative to reference geometry,
e_x – penalization value for x-th member elongation according to the given formula.

2.3.6. Ratio of bar lengths in consecutive iteration

Proportion of rod lengths addresses practical challenges of potential structures, caused by dynamic phenomena during movement. Therefore, it is essential to synthesize all other issues throughout the conceptual stage. Rod length proportion is an indicator of the approximate number of types of elements within the structural system that can be used to realize a physical model of a simulated structure according to maximal elongation of an individual bar at 1.15 of its initial length. Although it does not directly affect the quality of the structure, its analysis is closely related to the purpose of designing responsive structures as forms that effectively utilize their material and energy resources in line with current design trends according to trends described in [6].

$$\Delta d = \frac{d_{\max}}{d_{\min}}, \tag{17}$$

$$(\Delta d < 1.3), \quad f_x = \Delta d \cdot 100, \tag{18}$$

$$(1.3 \leq \Delta d), \quad f_x = \Delta d \cdot 1000, \tag{19}$$

$$f = \sum_{x=1}^{392} f_x, \tag{20}$$

$d_{\max}$ – length of the longest rod in the structure,
$d_{\min}$ – length of the shortest rod in the structure,
Δd – ratio of rod lengths (max/min),
f_x – bar length formula result for x-th member.

The profitability threshold was set at $\Delta d = 1.3$. Above this value, the number of different rods in the system increased to over 2, making the model inefficient to implement if diversity in strut types decreases material savings.

2.3.7. Intersection of upper and lower surfaces

Despite the authors implementing constraints on displacement of control points in the geometry to prevent self-intersections between upper and lower surfaces within the structure, completely avoiding this phenomenon would require implementation of complex mathematical formulas for structural movement. To simplify the problem, parameter for the intersection was included in the modification equation. In the Grasshopper model, a functional block checking for intersections between the upper and lower surfaces within the structure was present. It returned a positive value upon detecting a common curve or zero if there was no intersection. This value was then scaled so that all cases with incorrect geometry were deemed highly ineffective by the algorithm.

$$(\alpha \cup \beta = \emptyset) \quad \rightarrow \quad g = 0, \tag{21}$$

$$(\alpha \cup \beta \neq \emptyset) \quad \rightarrow \quad g = 1\,000\,000, \tag{22}$$

α – lower grid surface of the truss,
β – upper grid surface of the truss.

2.3.8. Final formula

After recalculating all partial optimization values, the algorithm sums them up to obtain a modification result. This result serves as an indicator of how efficiently the structure adheres to the geometric principles defined by mathematical formulas. Due to the mutual exclusivity of all parameters, a single strict optimization value cannot be achieved for all loading cases. Methods for evaluating the accuracy of results and predicting the algorithm's behavior are subject to further research not covered in this study.

Although all data are based on physical units, optimization results remain dimensionless. Physical units are multiplied by weight coefficients to achieve desired proportions of how several factors influence the final shape of the structure. Function is designed to clearly differentiate between solutions closer to optimal and less effective ones, thus requiring the function's susceptibility to a range of changes that the optimization algorithm may introduce. Final modification formula demonstrates satisfactory effectiveness. However, the open structure of the formula allows users to extend it with individual parameters relevant to individual structure, such as the tilt of elements, global curvature or curvature at measurement points on the surface, bending moments for bearing selection at joints, and similarly formulated components of final function.

Components of the modification formula are presented both as a summed result and in partial form as percentage contribution of each parameter to total modification result of a given iteration. This approach allows for examination of the relationship between shape and proportions of component sizes of the result. Additionally, linking percentage data with normalized charts for percentage-based data presentation enables tracking the history of changes in the structure from the start of the study to the point of finding modified geometry. This generates additional data that can be used to develop methods for predicting parts of results of individual studies.

In addition to the parameters included in the optimization formula, other key data are recorded for analyzing both individual models in terms of their efficiency and correctness, as well as for comparative purposes between successive geometry studies. A primary element of this analysis was measuring the depth of the truss at 49 uniformly spaced points as one of the main parameters involved in ensuring structure stiffness rigidity.

2.4. Evolution

Despite the complexity of the mathematical formula, the operation of the evolutionary algorithm is influenced directly only by the cumulative result of the function. Therefore, in addition to selecting parameters appropriate for the analysis, it was necessary to determine weighting coefficients that reflect the significance of each parameter for the result.

The evolutionary process begins with identifying initial relationships between input data and the resulting output. The algorithm iteratively adjusts the geometry based on its analysis of the result, triggering an update of the analysis, and providing a new output for the modification function. This iterative process generates a new set of analytical data for the algorithm. Such feedback creates a consistent trend of improvement in the modification function's result, typically reflected in its gradual reduction.

The evolution process can be terminated under several conditions: the passage of a predetermined time, the absence of result improvement within a specified period, or the achievement of a user-defined threshold. In this study, the authors opted for manual termination of the algorithm to determine a shorter operational time limit in which the most significant evolutionary changes occurred. After each experiment, the analysis data and study parameters were stored in a database included as an annex.

3. APPLICATION OF THE ALGORITHM

3.1. Challenges of implementing an evolutionary algorithm

As denoted in [27], formulating principles of structural movement is a strictly engineering issue that requires a methodical approach. It is based on optimization formulas seeking relationships between forces applied to structure (or a complex group of forces) and geometry that is most efficiently adapted to this load. In architecture and related fields, methods for moving structural elements, such as trusses or numerically controlled translation of shell supports, have been proposed. However, these methods have always been based on rigid algorithms with repeatable behaviors. Studies addressing such solutions have investigated individual computational models selected arbitrarily by the authors. Until now, models for modifying architectural responsive forms with more universal applications, which include the selection and formulation of criteria for structural movement, have not been explored.

To establish a method for formulating the behavior of movable structures, it was necessary to shift the approach from using pre-existing motion algorithms in favor of more natural form-seeking methods. A simple evolutionary algorithm was chosen, which, operating on its discrete modification mathematical model, seeks out the most efficient forms while receiving real-time progress data from consecutive iterations.

Primary issue with using an evolutionary algorithm arises from the nature of its calculations. Due to the usage of a blind trial method in the form-seeking process, the algorithm cannot control components influencing the optimization result. Additionally, by employing a pseudo-random method to study relationship between result and geometry, it cannot achieve the same result twice when repeating the process of shape generation. This inaccuracy causes a drift in form-seeking results and complicates further interpretation by automated systems that could support formulation of structural movement principles and behavior prediction. Repeatability, however, is achievable by implementing a function that records successive input data iterations generated by the algorithm, and artificially reproduces the process by following the resulting sequence of geometric changes. This method, while not precisely interpreting direction of evolution and lacking a rigidly defined goal, only has non-zero

chances of generating an optimal solution. However, the chance of finding a result close to the optimum increases significantly as the range of acceptable solutions is increased by minimally reducing its efficiency requirements. Nevertheless, it does not generate information about finding an effective extremum even after evaluating its value.

Therefore, it is necessary to precisely define the accuracy parameters for solving the geometry-generating problem or to introduce an additional result precision indicator that serves as a coefficient for weighted averaging of results. This is one of the objectives in exploring relationships between outcomes and obtained geometry.

The above-mentioned issue of data dimensionality in machine learning is closely related to functionality of the evolutionary algorithm. Research was conducted on a regular Intel Core-i7 9750H processor with a clock speed of 2.6GHz, using a portable personal computer, with additional parameters of 32GB RAM and offloading processor from generating graphics with a dedicated graphics card. The expected time for a single test to achieve a satisfactory form is 10 minutes. If only the evolutionary module is used without implementing machine learning, the number of tests would need to be increased by 3 orders of magnitude, significantly exceeding the computational power of currently available computers and the practicality of testing time. Usage of machine learning reduces work and power required to create a full behavior model or formulate the principle of geometry modification, but still requires creating a large set of tested solutions to train the algorithm, according to [27].

3.2. Preliminary research issues

When starting work on the model, it is crucial to define the algorithm's operating scheme, result precision and limitations, and to develop best practices for working with the model. This involves designing initial calibration studies for the object. Appropriate sequence of actions for calibrating the model includes:

- Studying model behavior during measurements: conducting a basic set of tests to determine overall efficiency of the algorithm.
- Studying result repeatability: determining maximum discrepancy in results for the same input data.
- Studying shape symmetry: assessing the algorithm's ability to identify basic dependencies based on the degree of similarity between the result and the most optimal symmetrical solution.
- Studying the impact of input data types on measurement outcomes: determining the rate of dependency of result for the same load case under varying initial geometry conditions.

4. STUDY OF MODEL BEHAVIOR DURING MEASUREMENT

Study of behaviors is based on a randomly selected representative group of loads (Fig. 5).

The study examines the functionality of the model. An additional parameter measured is efficiency of obtained forms. For calibration tests, 30 cases of concentrated forces, 6 cases of distributed forces simulating air pressure on the structure, 6 cases

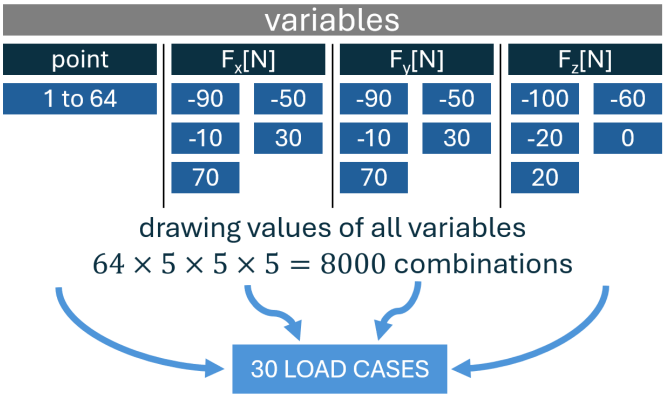

Fig. 5. Load case selection scheme for tests parameters randomization

of complex loads with multiple forces, and 3 combined cases consisting of both concentrated and distributed forces were chosen. The research group was selected randomly from all considered cases and diversified in terms of application of forces and components of their vectors. The research model is designed to adjust to diverse types of only static forces, including both point and surface forces, as well as uniform and non-uniform distributions. The load cases were selected from among all structural points defined as structure nodes without support nodes and within the range of forces: from −90 N to 70 N for horizontal components and from −100 N to 20 N for the vertical component. These ranges were then discretized into 40 N increments, yielding five potential values for each component. Simple load cases consisted of a single force, while complex cases involved 2 to 4 forces. Surface loads were selected from the same force pool but assumed to occur globally on the entire structure. Surface forces when applying are distributed on nodes proportionally based on the forces application area. All forces are assumed as applied in nodal points without any eccentricity. They involve only axial forces in structure members. The effect of dynamic actions was not considered and neither were strength issues related to the movement activity of the structure. All analyses were conducted with a nonlinear analysis module of Grasshopper Karamba 3D due to significant changes in the geometry of the model.

Each time before commencement of structure movement, the model is restored to reference geometry, normalizing the initial form of subsequent test trials. Using Galapagos evolutionary algorithm, studies are conducted. All test trials are solved by the program with identical algorithm operating parameters. Time for a single modification is set to 10 minutes.

4.1. Course of the study

In the first stage, 30 test studies are conducted. All cases result in obtaining geometries more efficient than the initial model. During the 10 minutes allocated for each study, approximately 1100 configurations are analyzed for each study. Progress of studies is continuously monitored by observing the shapes of generated structures.

4.2. Result

Optimization result satisfactorily fulfills its function, and straightforward operation formula allows for detecting behavioral tendencies. In the initial phase of the study, when the algorithm tests directions for further evolution, the score increases to maximum recorded values, oscillating around $5 \cdot 10^6$ points. This is related to starting the study with high values of input parameters, which are non-optimal for the tested structure according to inefficient load distribution. On average, after 1 minute, efficiency in lower configurations is recognized, and the algorithm rejects upper values of variables "a" to "g" as it is defined in Fig. 6 as stage 1. Gradual physical flattening of the structure (by lowering B, D, F, H, B′, D′, F′, H′ values) is related to minimizing the overall formula score, radically changing proportions of "a" to "g" components in the optimization result. This stage 2 lasts about 1.5 minutes, during which final component proportions are formed. Although the resulting shapes are still inefficient, they remain in the range of 150 000 to 450 000 final formula points. The last stage of stabilizing geometry changes focuses on maintaining proportions of elements. Still high contribution of the "rod extension $-e''$ component is compensated by reducing truss depth from an average of 1.1/1.15 m to 0.85/0.91 m. Although all "genes" of the algorithm are equally subject to continuous modifications, it is observed between successive iterations that heights of points B, D, F, H regularly return to values from the beginning of stage 3, as presented in Fig. 7, as minimal deviations of parameters in individual iterations, while parameters B′, D′, F′, H′, all defined in Fig. 2 in the "2.1. Geometry" section undergo constant modification.

During each test run, a consistent trend of achieving similar share of parameters in the final formula is observed (Fig. 6). Its

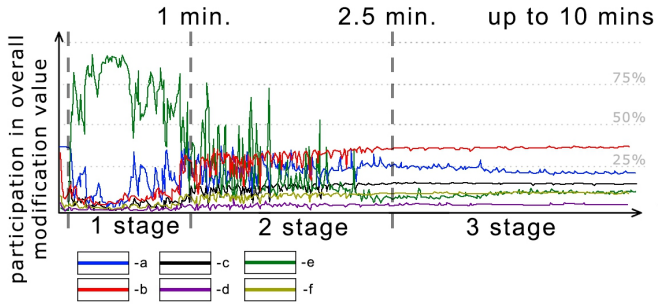

Fig. 6. Diagram showing what share each coefficient had in the result of the modification function. For example, in the middle of stage 1, coefficient "b" accounted for about 8–9% of the result of the modification function. By the end of the study, it accounted for 37% of the result

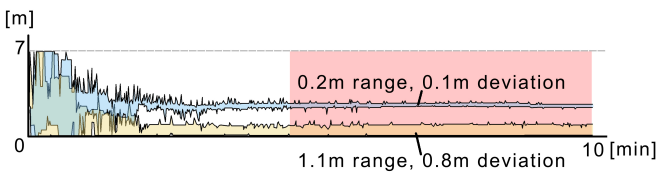

Fig. 7. Example graph of parameters B, D, F, H (blue) and B′, D′, F′, H′ (yellow) height ranges, showing the initial disorder of the search for the form and further repeatable values

share degree reflects the impact of individual parameters on the final formula – the higher the percentage in the final solution, the larger the influence of the geometry parameter.

In data structure of the results, similarities in proportions of the components can be found. Initially, in the vast majority of studies, the most significant component is the extension of the rods. Until the end of the first phase, this retains a share of the final formula at 98.7%. Then, during lowering physical height of the structure, it drops to 91.5–93.4%. In the final stage, when the algorithm recognizes the potential to reduce results with this parameter, a significant reduction occurs to about 2.1–5.1%, though it still exceeds this value for proportionally larger forces. Overall, the general trend shows value drop in stage 3 from 91% to 5%. Rod extension coefficient introduces the most noticeable changes in the modification formula. Limiting rod extension according to the described formula results in maximum extension of rod in the 27th study reaching a value of 1.1499, staying at the boundary of the highest degree of structure penalization – 1.15 according to (formula (16)). Conversely, the greatest shortening recorded for the 28th study is 0.87 of the original length, also approaching the limit of advantageous extension set at 0.85 according to (formula (10)).

Individual peaks of values in the final formula values history during the study provide information about sensitivity of applied modification formula to minimal changes. These peaks result from exceeding the efficiency or serviceability limits of the structure, which according to the model design, excludes a given iteration from further efficiency studies. The final optimization result ranges between 21 038 and 46 714 points while resultant geometry appears similar to the initial one (Fig. 7), but this value does not serve as a basis for comparison of research results among themselves. For comparative purposes, elementary values can be used such as the reduction of deflection, extension or shortening of rods, and stress distribution parameter so as raw components of the equation.

Deformation parameter is satisfactory, thus constituting a minimal influence of the result from the beginning of each study up to the final solution. From the beginning of the second phase, marginal contribution of deformation becomes more influential, immediately assuming a stable range of 25.5–45.6% of overall final formula value. All final values of the parameter fall within this range. For each iteration in every study, the program compares current deflection of the structure to the maximum value defined as 1/300 of the span equal to 3.33 cm. The deformations obtained are significantly below the usability limit, confirming the algorithm's ability to enhance the usability limit of the structure. Deflection arrows range from 0.04 cm to 0.25 cm (Table 1). The average deflection value for the reference structure in a set of 30 test trials is 0.1609 cm. Using the geometry modification model described allows for minimization of this value to 0.1064 cm, increasing efficiency of the structure by nearly 34%.

Maximum utilization of elements should be referred to the proportion of minimum to maximum utilization. Changes in both values show a significant similarity in variations and a diverse impact on the result according to the participation proportions designed. Both coefficients achieve the most stable final values, which are, respectively, 18.7–19.3% of the result

Table 1
Summary of key data from the first measurements of the structures. In each case, improvements in geometry efficiency are evident

	Case 1	Case 2	Case 3	Case 4	Case 5	Case 6	Case 7	Case 8
Force position X	4.28571	1.4285	0	6.42857	0	1.42857	4.28571	2.14286
Force position Y	2.85714	7.1428	7.14286	2.14286	4.28571	2.85714	4.28571	9.28571
Result	28733.3	32082.4	25234.2	23115.4	34105.3	27890.7	29925.9	24534.4
Displacement	0.11976	0.15453	0.09414	0.08929	0.18138	0.11308	0.1393	0.09358
f_x [N]	70	30	30	–90	–10	30	–10	70
f_y [N]	30	–50	–90	–50	70	–90	30	–10
f_z [N]	–60	20	0	–100	20	0	–60	–20
f [N]	96.95	61.64	94.87	143.53	73.48	94.87	67.82	73.48
B [m]	2.96	3.15	2.69	3.41	4.24	3.66	2.60	3.92
D [m]	2.44	2.56	2.43	3.44	2.75	3.18	2.74	3.07
F [m]	1.64	2.88	3.56	3.46	2.66	2.56	3.58	2.46
H [m]	3.00	3.83	3.19	3.351	2.60	2.63	2.52	2.72
B′ [m]	0.86	0.89	0.98	0.89	0.82	0.60	1.16	0.86
D′ [m]	0.96	0.85	1.09	1.05	1.14	0.95	0.68	0.93
F′ [m]	1.22	1.00	0.93	0.86	0.73	0.98	1.24	0.91
H′ [m]	1.03	1.01	0.93	1.08	1.19	1.113	0.95	0.99
Result	28052.55	27763.83	24265.21	21049.43	26792.90	26363.12	25721.37	22238.30
Mass [kg]	7690.78	7664.51	7701.04	7744.62	7701.82	7623.24	7722.52	7636.88
Maximal displacement [m]	0.10	0.10	0.07	0.05	0.09	0.08	0.08	0.05
Utilization min [%]	0.52	0.65	0.54	0.36	0.43	0.66	0.51	0.71
Utilization max [%]	6.38	4.92	5.61	2.6	5.09	5.24	4.63	3.79
Utilization min/max	12.32	7.56	10.32	7.17	11.72	7.90	9.12	5.16
Max bar shortening	0.94	0.92	0.94	0.92	0.91	0.91	0.90	0.93
Max bar elongation	1.10	1.10	1.07	1.09	1.12	1.06	1.10	1.09
Elongation ratio	1.16	1.20	1.14	1.18	1.23	1.16	1.22	1.18
Min bar length [m]	1.04	1.01	1.02	1.01	1.01	1.02	1.02	1.01
Max bar length [m]	1.90	2.00	1.97	2.02	2.00	1.92	1.98	1.97
Length ratio in this iteration	1.83	1.97	1.93	2.00	1.98	1.89	1.93	1.94

for “maximum utilization” and a range of 3.50–3.74 for the “min/max” ratio (Table 1).

During the evolution process, it was not possible to distinguish the periods when these indicators dominated the truss shape modification process. Utilization ratio indicator remained the most varied among the result components, with minimum values ranging from 0.3% to 1% and maximum values – from 2.5% to 10% (Table 1).

This means that the structure was significantly over-dimensioned. However, this did not complicate structural analysis but only provided information that such a structure could be optimized in terms of own weight.

4.3. Relationship studies between component parameters and adjustment of the result

The second stage of building the mathematical formula for geometry modification aims to increase effectiveness of the evolutionary algorithm in recognizing results in vicinity of the optimal value. Such staging of work is characteristic of the processes and methodologies for developing modification metamodels, and it has been applied in the case being analyzed to develop an effective function for motion modeling. Galapagos algorithm selects input values based on comparisons of results among themselves at each subsequent measurement, striving to significantly reduce the range of values being searched. This approach carries the

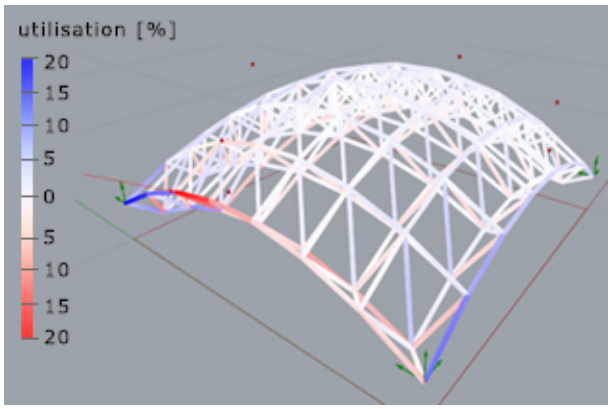

(a)

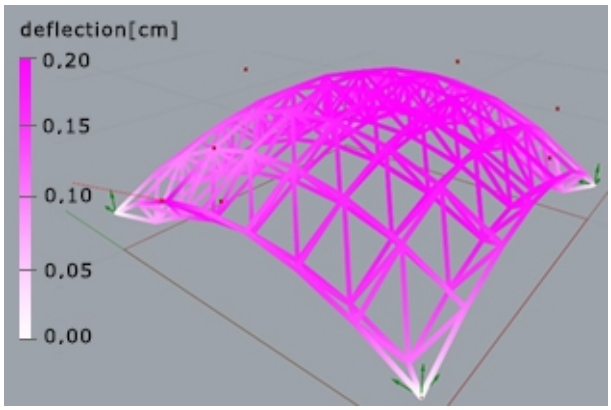

(b)

Fig. 8. (a) presentation of the degree of elements utilizations, (b) presentation of displacements

risk that the program might identify a local minimum of the optimization function as the global minimum. This risk increases with greater fluctuations in the final function (Fig. 9).

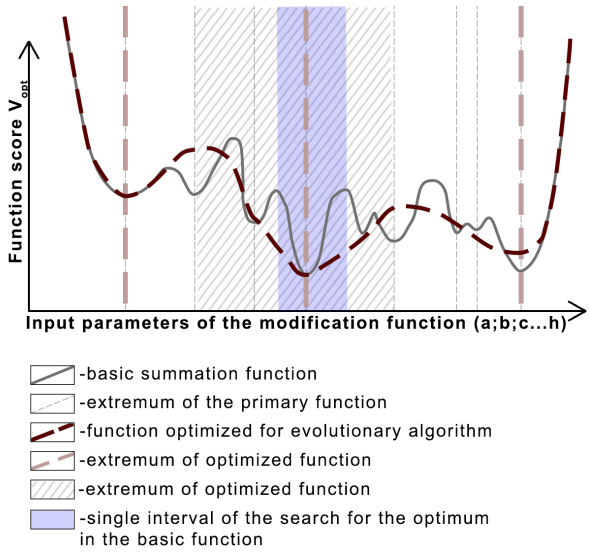

Fig. 9. Diagram of the progression of a primary function with multiple local extrema, and a modified function with a reduced number of extrema

To mitigate the impact of this phenomenon on the model's efficiency, the authors performed a manual analysis of results from a structure based on basic summation formula V_{opt}. By identifying trends, similarities and proportional relationships among resulting values, the final formula was modified to align with operational characteristics of the evolutionary algorithm. This adjustment, while expanding the search range, reduces the risk of the algorithm becoming stuck in an inefficient range.

The correlation study began with simple linear relationships using the Pearson's method. No correlation was found between force vectors and partial results, with Pearson coefficient reaching a maximum of 0.314. However, several significant interdependencies among the components were observed, as shown in Table 2.

Table 2
Pearson's correlation matrix between the proportions of component contributions to the score

	a	b	c	d	e	f
a		–0.95667	–0.35399	–0.1797	0.636072	0.990427
b	–0.95667		0.152723	–0.07229	–0.69804	–0.95594
c	–0.35399	0.152723		–0.51811	–0.49165	–0.38277
d	0.179702	–0.07229	–0.51811		0.043465	0.174213
e	0.636072	–0.69804	–0.49165	0.043465		0.688121
f	0.990427	–0.95594	–0.38277	0.174213	0.688121	

Strong dependencies were noted for parameters a–b, a–f, and b–f. In the first case, there is an inverse relationship. This relationship is described by the following formula:

$$55.57\%V_{\text{opt}} < a + b < 70.57\%V_{\text{opt}}\,. \tag{23}$$

The strongest simple correlation between a and f explains the inclusion of a relationship between these two variables in the final formula:

$$\frac{f}{a} \approx 4.01. \tag{24}$$

The most consistent component in the result is the "c" parameter – maximum cross-sectional utilization. Oscillating around an average share of 19.75%, it ranges from 14.87% to 25.94%. Its stability in the solution is captured in the formula by defining a convergent point in a quadratic function.

The weight and extension parameters of the rods, being interdependent, can be considered in calculations based on the principle of increased instability of the structure with changes in its weight. Decreasing or increasing mass causes rods to operate in an unexamined range of behaviors, which generates the risk of nonlinearity in the telescopic mechanism's performance.

Deflection and effective cross-sectional utilization, being the most critical geometry modifier parameters, have the greatest impact on the result of the formula. The formula incorporating dependencies between variables identified in the second stage

takes the following form:

$$V_{\text{opt}_{\text{mod}}} = \left(\left(1+\frac{|a-7650|}{100}\right)e+\left(\left(\frac{c}{\sum_{a=i}^{f} x_i}-19.75\right)^2+1\right)c + f\left(\left|\frac{f}{a}-4.01\right|+1\right)\right)\cdot\sqrt{bd\cdot 1^{-6}}+g. \quad (25)$$

4.4. Effect of formula modification on geometry generation efficiency

The equation developed, optimized for use by the evolutionary algorithm, undergoes performance testing. It is examined for the speed of generating solutions more effectively than the reference model and effectiveness of obtained forms as compared with the non-optimized criterion summation function.

Comparative test results on an identical group of 30 static configurations show a distinctive character of the function from its unmodified form. In most cases, the algorithm achieved results that were on average 12.91% to 19.06% worse. Only in 4 trials did the results outperform the unmodified form, which disqualifies the equation as a standalone method for managing geometry modifications. However, it still produced better results than the unmodified structure and generated more effective forms, on average 1.6 times faster than the unmodified function. This justifies the use of a hybrid two-stage modification approach, where the first stage employs the modified algorithm $V_{\text{opt}_{\text{mod}}}$, and in the second stage, shape modification continues using the V_{opt} algorithm based on the already collected data.

4.5. Dependences and trends

To leverage machine learning for accelerating structural shaping, a sufficiently large dataset is necessary. Given the need to control 8 parameters relative to several outcome values, the research group expands by orders of magnitude, making machine learning implementation infeasible at this stage. The series of tests was designed to reveal basic relationships in successive measurements. Understanding these correlations can help adjust the model for earlier use of computational power in speeding up research.

A random sample of applied forces includes cases of concentrated forces ranging from 14.14 kN to 161.86 kN. The algorithm can optimize shapes to varying degrees, but with 100% effectiveness, it found more efficient configurations than the reference model using V_{opt} and $V_{\text{opt}_{\text{mod}}}$. Reduction in deflection was always above 12.86%, with an average of 33.02% and a maximum reduction in vertical displacement of 51.22%. The degree of optimization does not significantly correlate with the applied force value or components of the force vector. However, there is convergence with the point of force application and the value of deflection reduction. For forces applied at the edge nodes of the structure, the algorithm consistently finds twice as efficient shapes, reducing deflection in the range of 51.22% to 46.34% for forces applied closer to the center of span and in the range of 27.02% to 18.29% closer to supports. Lower optimization results for the second group of the cases are simply due to the smaller base deflections of elements closer to supports and a smaller range of movement of points in that vicinity.

A more complex dependency is also observed. For points closer to the center of the structure, the reduction in the optimization result is like reduction in deflection. It is noted that as the distance of the force application point from the center of the structure increases and as the angle between the vertical reference vector and vector of the applied force increases, proportion of the result to deflection loses correlation. This is because the shape modification model based on the evolutionary algorithm benefits from absence of constraints such as rigid weighting coefficients in the shaping process. This means that longer operation of the algorithm during a single test balances effective contribution of component coefficients to the final result. This deviation from previous research approaches to the issue of movement in architecture results in more flexible generation of solutions, increasing the range of acceptable geometries, and thus allowing the algorithm a larger margin of error – if there are more solutions considered close to the optimal one, it is easier for the program to find one of them.

5. CONCLUSIONS

5.1. Parameter ranges of "genes"

The initially applied range of parameters defined for the evolutionary algorithm, referred to as "genes", is too wide. The effective range of solutions for the tested series is between 1.017 m and 4.239 m for the lower grid and 0.574 m to 1.499 m for the upper grid. Given that tests were conducted with non-maximum applied forces in random locations rather than potentially critical points, it is necessary to narrow the search range for the shape to 0.6 m–5.5 m in the lower grid and 0.3 m to 1.9 m in the upper grid for single force configurations. Proportional consideration should be given to more complex loading scenarios and their range values should be revised. These constraints will significantly improve the efficiency of shape searching and reduce the time for a single test. The range of optimal value searches for single-force load cases is thus reduced by several orders of magnitude.

5.2. Evolutionary algorithm

Initially, in the function responsible for intersecting two surfaces, the penalty value for detecting an intersection was set to $g = \infty$. During measurements, it was observed that the algorithm had issues using infinity to relate efficiency with the shape. Galapagos interpreted geometries with an infinite value as exceptionally inefficient. Consequently, it also deemed the forms in the large vicinity of the detected value as inefficient, blocking further testing of these forms (Fig. 10). As a result, it consistently blocked the vicinity of the optimal result and hindered its correct operation, yielding increasingly poorer forms with subsequent iterations. A revised penalty value of $g = 1\,000\,000$ was introduced, which resolved the issue of interpreting the vicinity of incorrect geometry, allowing the search for efficient shapes even after an iteration with an intersection.

The algorithm consistently attempted to reduce the result by lowering the currently highest parameter in each case studied.

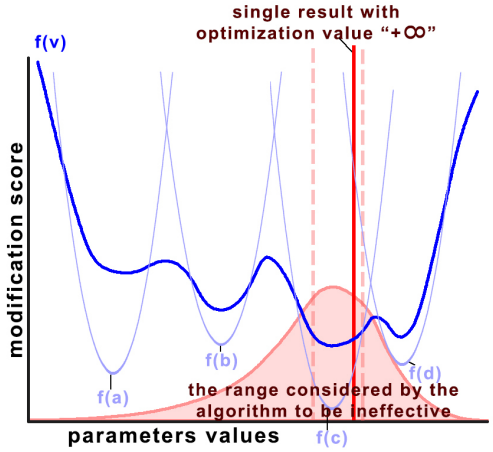

Fig. 10. The program stops working properly after a modification result equal to + infinity

Whenever all contributing parameters were reduced, subsequent iterations of this action yielded progressively smaller effects. Each time, the reduction was at least an order of magnitude smaller. After the second phase, described in the "Results" section, stabilization occurred. By determining optimal distribution of the proportions, it is possible to develop a method for assessing when the algorithm has satisfactorily approached the optimal value. This allows for dynamic control of search time for optimal form, tailored to the specific study and current progress of the program.

5.3. Summary

The presented method of structural design using parametric modeling and implementation of custom geometric evolution constraints yields noticeably improved results. It can effectively serve as foundation for a responsive structural behavior model, assuming influence of low dynamic force changes (such as snow, rain, and user loads). This approach can significantly enhance the serviceability limit of a structure.

Changes introduced to the shape modification equation after initial series of studies positively impact efficiency of searching for optimal structural forms, reducing computational time needed to achieve better results.

The model enables automation of the structure's movement control process while maintaining full access to modifiable criteria for directing the evolutionary algorithm. This approach also ensures the ability to generate a wide variety of change records and outcomes, continuously building a growing database for reinforcement learning (RL).

5.4. Further research

Subsequent stages of calibration, based on principles derived from the first series of studies, can serve as input data for creating a machine learning model and for investigating methods for immediate response upon detecting a force, even before shape analysis by the evolutionary algorithm is conducted. After completing all planned tests, the process of collecting results from a wide range of cases should begin. This data will form the foundation for developing simple and more complex protective behavior models and machine learning, starting with the interpolation of cases involving a single force at one node, on one line, within a complex loading scenario, and then seeking correlations for more varied cases.

At each stage, the algorithm should be monitored and its metaparameters adjusted to achieve the best possible results. The outcomes obtained will then be subject to validation. This process aims to improve the model's effectiveness in responding to external forces and their changes.

Further research should focus on:

- further improvement of efficiency of solutions;
- increasing the accuracy of the study by implementing in the mathematical formula further variables relating to the problems of analysis, execution and use of the structure;
- developing a database of already obtained results for use as an additional source of information on effective geometries;
- analyzing the conditions and requirements that the spatial structural system selected for the model should meet.

REFERENCES

[1] N. Negroponte, *Soft Architecture Machines*. 1976, doi: 10.7551/mitpress/6317.001.0001.

[2] T.D.E. Sterk, "Building upon Negroponte: a hybridized model of control suitable for responsive architecture," *Autom. Constr.*, vol. 14, no. 2, pp. 225–232, Mar. 2005, doi: 10.1016/J.AUTCON.2004.07.003.

[3] T. Herdt, "From cybernetics to an architecture of ecology: Cedric price's interaction centre," *Footprint*, vol. 15, no. 1, pp. 45–62, 2021, doi: 10.7480/footprint.15.1.4946.

[4] M. Meagher, "Designing for change: The poetic potential of responsive architecture," *Front. Archit. Res.*, vol. 4, no. 2, pp. 159–165, 2015, doi: 10.1016/j.foar.2015.03.002.

[5] A. Menges and S. Reichert, "Performative wood: Physically programming the responsive architecture of the HygroScope and HygroSkin projects," *Archit. Des.*, vol. 85, no. 5, pp. 66–73, 2015, doi: 10.1002/ad.1956.

[6] A.P. Reksowardojo, G. Senatore, and I.F.C. Smith, "Experimental testing of a small-scale truss beam that adapts to loads through large shape changes," *Front. Built Environ.*, vol. 5, p. 93, 2019, doi: 10.3389/fbuil.2019.00093.

[7] Y. Wang, X. Xu, and Y. Luo, "Minimal mass design of active tensegrity structures," *Eng. Struct.*, vol. 234, p. 111965, 2021, doi: 10.1016/j.engstruct.2021.111965.

[8] J.L. Wagner *et al.*, "Optimal Static Load Compensation With Fault Tolerance in Nonlinear Adaptive Structures Under Input and State Constraints," *Front. Built Environ.*, vol. 6, p. 93, 2020, doi: 10.3389/fbuil.2020.00093.

[9] A.P. Reksowardojo, G. Senatore, A. Srivastava, C. Carroll, and I.F.C. Smith, "Design and testing of a low-energy and -carbon prototype structure that adapts to loading through shape morphing," *Int. J. Solids. Struct.*, vol. 252, p. 111629, 2022, doi: 10.1016/j.ijsolstr.2022.111629.

[10] M.C. Phocas, "Interdisciplinary Research-based Design: the Case of a kinetic form-active Tensile Membrane," *J. Archit. Eng. Technol.*, vol. 01, no. 02, pp. 1–7, 2012, doi: 10.4172/2168-9717.1000104.

[11] C. Kelleter, T. Burghardt, H. Binz, L. Blandini, and W. Sobek, "Adaptive Concrete Beams Equipped With Integrated Fluidic Actuators," *Front. Built Environ.*, vol. 6, p. 91, 2020, doi: 10.3389/fbuil.2020.00091.

[12] A. Warsewa *et al.*, "Self-tuning state estimation for adaptive truss structures using strain gauges and camera-based position measurements," *Mech. Syst. Signal Process.*, vol. 143, p. 106822, 2020, doi: 10.1016/j.ymssp.2020.106822.

[13] G. Senatore, P. Duffour, and P. Winslow, "Synthesis of minimum energy adaptive structures," *Struct. Multidiscip. Optim.*, vol. 60, no. 3, pp. 849–877, 2019, doi: 10.1007/s00158-019-02224-8.

[14] A.P. Reksowardojo, G. Senatore, and I.F.C. Smith, "Actuator layout optimization for adaptive structures performing large shape changes," in *Lecture Notes in Computer Science (including subseries Lecture Notes in Artificial Intelligence and Lecture Notes in Bioinformatics)*, 2018, pp. 111–129, doi: 10.1007/978-3-319-91638-5_6.

[15] M.A. Zboinska, J. Cudzik, R. Juchnevic, and K. Radziszewski, "A Design Framework and a Digital Toolset Supporting the Early-Stage Explorations of Responsive Kinetic Building Skin Concepts," in *Proceedings of the International Conference on Education and Research in Computer Aided Archit. Des. in Europe*, 2015, pp. 715–725, doi: 10.52842/conf.ecaade.2015.2.715.

[16] M. Senagala, "Kinetic, Responsive and Adaptive: a Complex-Adaptive Approach To Smart Architecture," *SIGRADI 2005 International Conference*, 2005, Peru.

[17] V. Temporin, J. Volpato, P.L. Cocco, A. D'Angelo, and M. Tieghi, "Time enhanced architectural modelling (T.E.A.M.): Virtual reality project for the planning and visualization of kinetic architecture and dynamic design," in *J. Phys.-Conf. Ser.*, 2021, p. 012072, 2021, doi: 10.1088/1742-6596/2042/1/012072.

[18] R. Dörrie *et al.*, "Automated force-flow-oriented reinforcement integration for Shotcrete 3D Printing," *Autom. Constr.*, vol. 155, p. 105075, 2023, doi: 10.1016/j.autcon.2023.105075.

[19] L. Kabošová, E. Kormaníková, S. Kmeť, and D. Katunský, "Shape-changing tensegrity-membrane building skin," *MATEC Web Conf.*, vol. 310, p. 00046, 2020, doi: 10.1051/matecconf/202031000046.

[20] R.A. Danhaive and C.T. Mueller, "Combining parametric modeling and interactive optimization for high-performance and creative structural design," *Proc. International Association for Shell and Spatial Structures (IASS) Symposium 2015*, Netherlands, Aug. 2015, pp. 1–11.

[21] T. Wortmann, "Genetic evolution vs. function approximation: Benchmarking algorithms for Archit. Des. optimization," *J. Comput. Des. Eng.*, vol. 6, no. 3, pp. 414–428, 2019, doi: 10.1016/j.jcde.2018.09.001.

[22] A. Kaveh and M.I. Ghazaan, *Meta-heuristic algorithms for optimal design of real-size structures*. Springer Cham, 2018, doi: 10.1007/978-3-319-78780-0.

[23] H. Adeli and K.C. Sarma, *Cost Optimization of Structures: Fuzzy Logic, Genetic Algorithms, and Parallel Computing*. John Wiley & Sons, Ltd, 2006, doi: 10.1002/0470867353.

[24] K.D. Tsavdaridis, E. Efthymiou, A. Adugu, J.A. Hughes, and L. Grekavicius, "Application of structural topology optimisation in aluminium cross-sectional design," *Thin-Walled Struct.*, vol. 139, pp. 372–388, 2019, doi: 10.1016/j.tws.2019.02.038.

[25] G. Senatore and A.P. Reksowardojo, "Force and Shape Control Strategies for Minimum Energy Adaptive Structures," *Front. Built Environ.*, vol. 6, p. 105, 2020, doi: 10.3389/fbuil.2020.00105.

[26] J. Chilton, *Space Grid Structures*. Taylor & Francis Group, 2007, doi: 10.4324/9780080498188.

[27] O.Y. Al-Jarrah, P.D. Yoo, S. Muhaidat, G.K. Karagiannidis, and K. Taha, "Efficient Machine Learning for Big Data: A Review," *Big Data Res.*, vol. 2, no. 3, pp. 87–93, Apr. 2015, doi: 10.1016/j.bdr.2015.04.001.